





































An Updated Detection Pipeline for Precursor Emission in Type II Supernova 2020tlf

W. V. JACOBSON-GALÁN ^{1,2}, L. DESSART ³, D. O. JONES ⁴, R. MARGUTTI ⁵, D. L. COPPEJANS ⁶, G. DIMITRIADIS ⁷,
R. J. FOLEY ⁸, C. D. KILPATRICK ⁶, D. J. MATTHEWS ⁵, S. REST ⁹, G. TERRERAN ¹⁰, P. D. ALEO ^{11,12}, K. AUCHETTL ^{13,14,8,15},
P. K. BLANCHARD ⁶, D. A. COULTER ⁸, K. W. DAVIS ⁸, T. J. L. DE BOER ¹⁶, L. DEMARCHI ⁶, M. R. DROUT ¹⁷, N. EARL ¹¹,
A. GAGLIANO ^{11,12}, C. GALL ¹⁵, J. HJORTH ¹⁵, M. E. HUBER ¹⁶, A. L. IBIK ¹⁷, D. MILISAVLJEVIC ¹⁸, Y.-C. PAN ¹⁹,
A. REST ^{20,9}, R. RIDDEN-HARPER ²¹, C. ROJAS-BRAVO ⁸, M. R. SIEBERT ⁸, K. W. SMITH ²², K. TAGGART ⁸, S. TINYANONT ⁸,
Q. WANG ⁹ AND Y. ZENATI ⁹

¹Department of Astronomy and Astrophysics, California Institute of Technology, Pasadena, CA 91125, USA

²NASA Hubble Fellow

³Institut d'Astrophysique de Paris, CNRS-Sorbonne Université, 98 bis boulevard Arago, F-75014 Paris, France

⁴Institute for Astronomy, University of Hawai'i, 640 N. A'ohoku Pl., Hilo, HI 96720, USA

⁵Department of Astronomy and Astrophysics, University of California, Berkeley, CA 94720, USA

⁶Center for Interdisciplinary Exploration and Research in Astrophysics (CIERA), and Department of Physics and Astronomy, Northwestern University, Evanston, IL 60208, USA

⁷School of Physics, Trinity College Dublin, The University of Dublin, Dublin, Ireland

⁸Department of Astronomy and Astrophysics, University of California, Santa Cruz, CA 95064, USA

⁹Department of Physics and Astronomy, The Johns Hopkins University, Baltimore, MD 21218, USA

¹⁰Las Cumbres Observatory, 6740 Cortona Dr, Suite 102, Goleta, CA 93117-5575, USA

¹¹Department of Astronomy, University of Illinois at Urbana-Champaign, 1002 W. Green St., IL 61801, USA

¹²Center for Astrophysical Surveys, National Center for Supercomputing Applications, Urbana, IL, 61801, USA

¹³School of Physics, The University of Melbourne, VIC 3010, Australia

¹⁴ARC Centre of Excellence for All Sky Astrophysics in 3 Dimensions (ASTRO 3D)

¹⁵DARK, Niels Bohr Institute, University of Copenhagen, Jagtvej 128, 2200 Copenhagen, Denmark

¹⁶Institute for Astronomy, University of Hawaii, 2680 Woodlawn Drive, Honolulu, HI 96822, USA

¹⁷David A. Dunlap Department of Astronomy and Astrophysics, University of Toronto, 50 St. George Street, Toronto, Ontario, M5S 3H4, Canada

¹⁸Department of Physics and Astronomy, Purdue University, 525 Northwestern Avenue, West Lafayette, IN 47907, USA

¹⁹Graduate Institute of Astronomy, National Central University, 300 Zhongda Road, Zhongli, Taoyuan 32001, Taiwan

²⁰Space Telescope Science Institute, Baltimore, MD 21218

²¹School of Physical and Chemical Sciences — Te Kura Matū, University of Canterbury, Private Bag 4800, Christchurch 8140, New Zealand

²²Astrophysics Research Centre, School of Mathematics and Physics, Queen's University Belfast, Belfast BT7 1NN, UK

1. SUPPLEMENTARY FIGURES & DATA

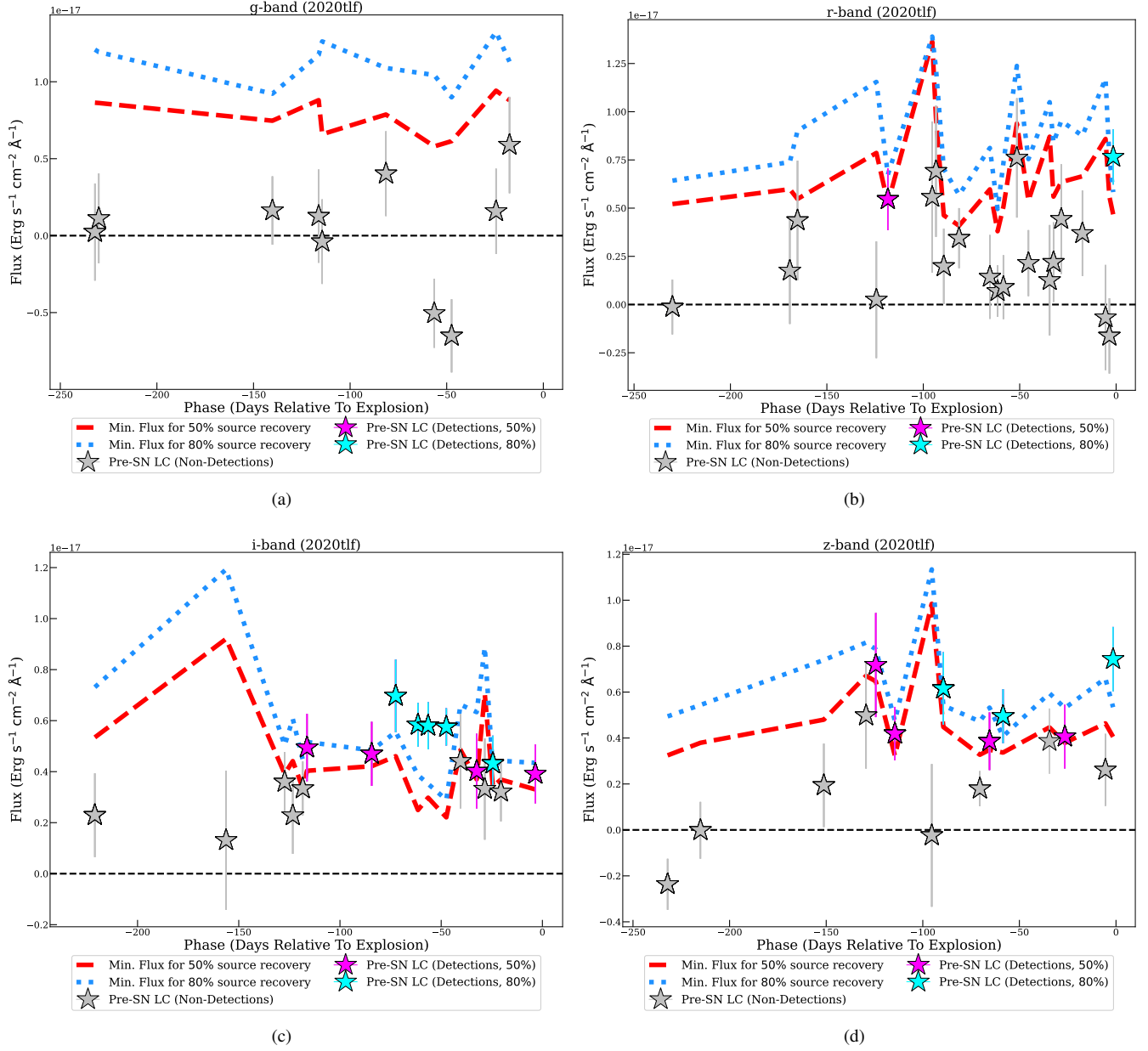


Figure 1. Pre-explosion *griz*-band light curve of SN 2020tlf. Detections above 80% and 50% recovery levels shown as cyan and magenta stars, respectively. Calculated flux at the SN location that is below these recovery levels is shown as grey stars. Minimum fluxes for 80% and 50% injected source recovery shown as blue dotted and red dashed lines, respectively.

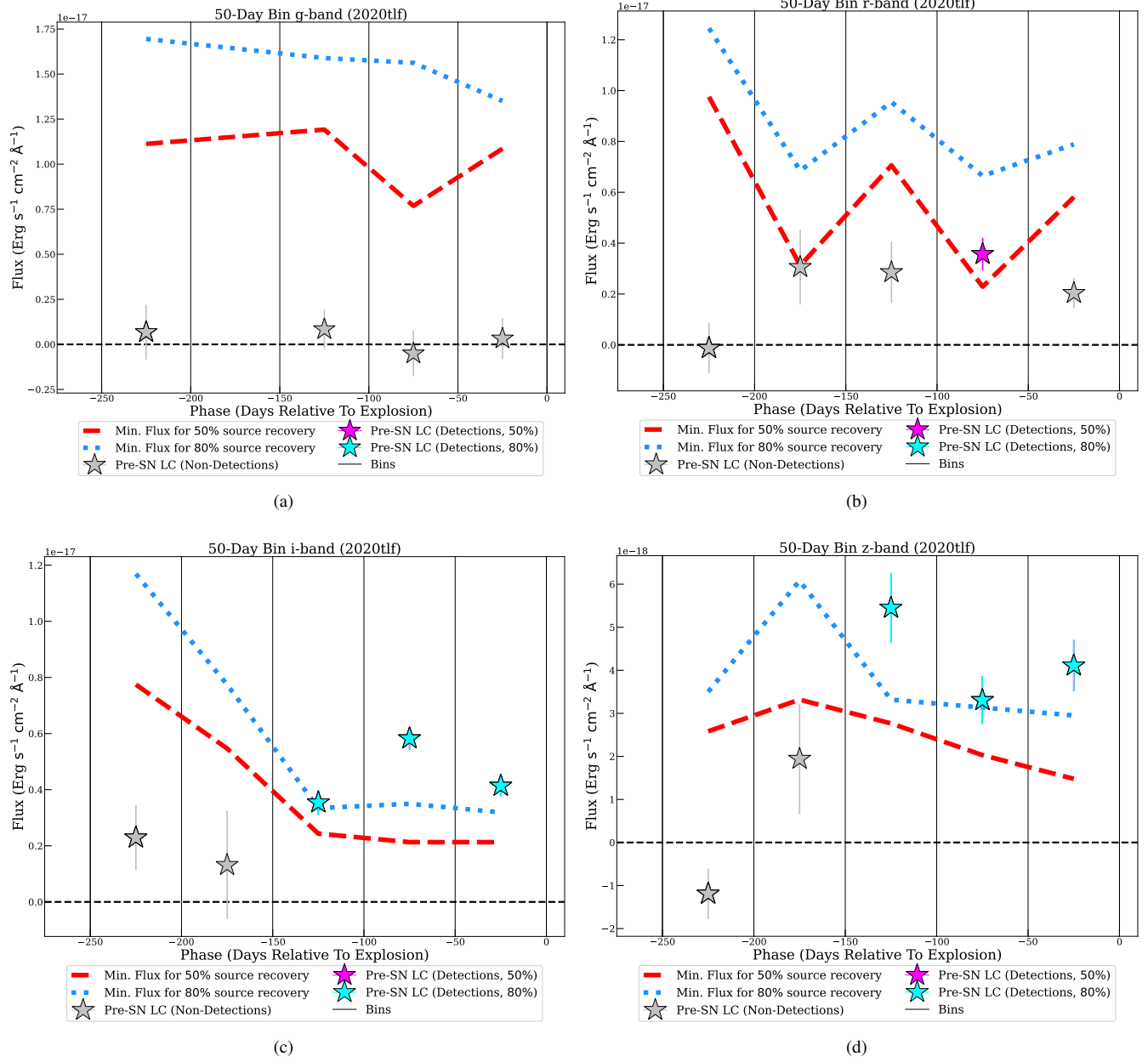


Figure 2. Pre-explosion *griz*-band light curve of SN 2020tlf where the flux has been stacked in 50 day bins. Detections above 80% and 50% recovery levels shown as cyan and magenta stars, respectively. Calculated flux at the SN location that is below these recovery levels is shown as grey stars. Minimum fluxes for 80% and 50% injected source recovery shown as blue dotted and red dashed lines, respectively.

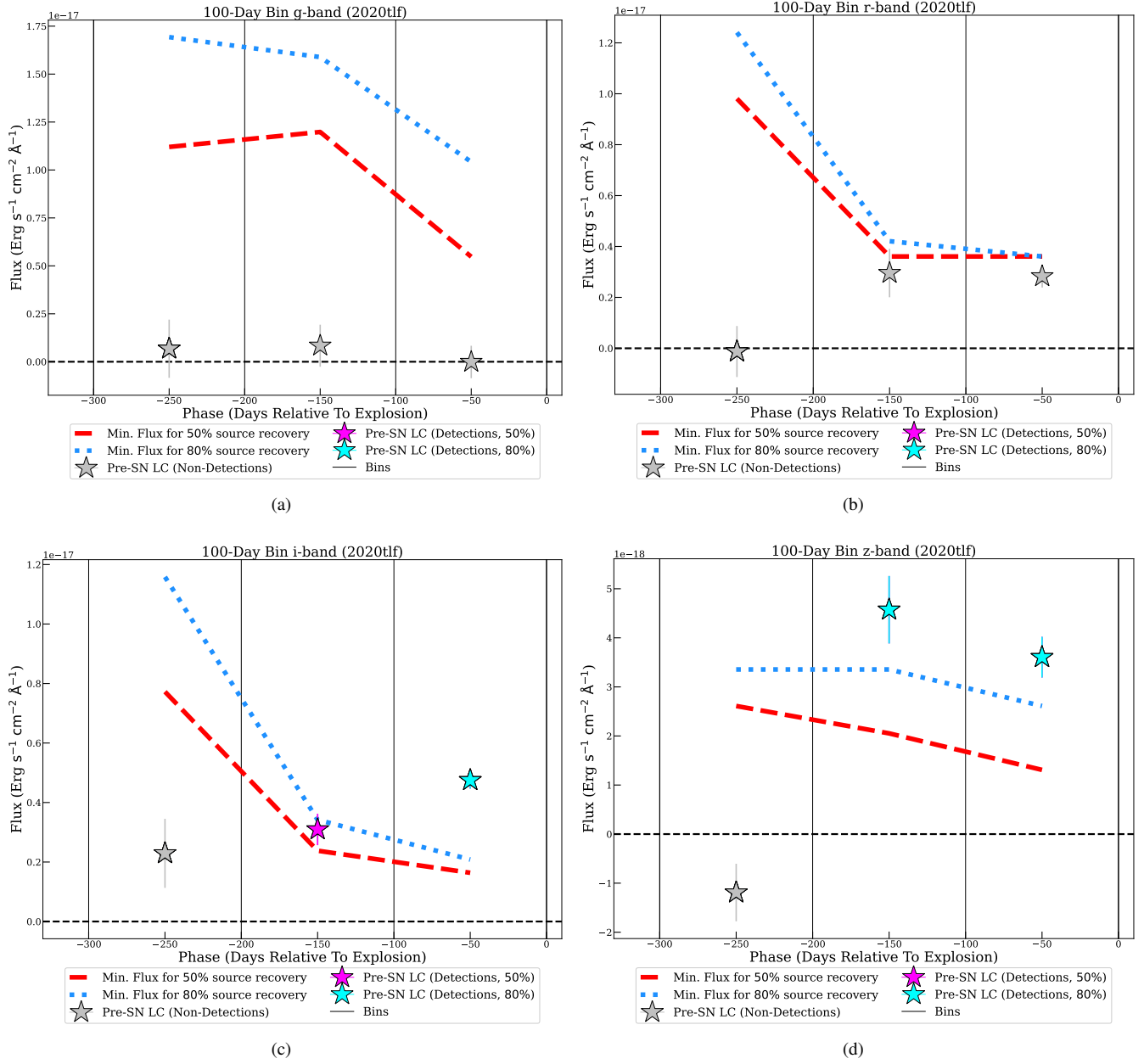


Figure 3. Pre-explosion *griz*-band light curve of SN 2020tlf where the flux has been stacked in 100 day bins. Detections above 80% and 50% recovery levels shown as cyan and magenta stars, respectively. Calculated flux at the SN location that is below these recovery levels is shown as grey stars. Minimum fluxes for 80% and 50% injected source recovery shown as blue dotted and red dashed lines, respectively.

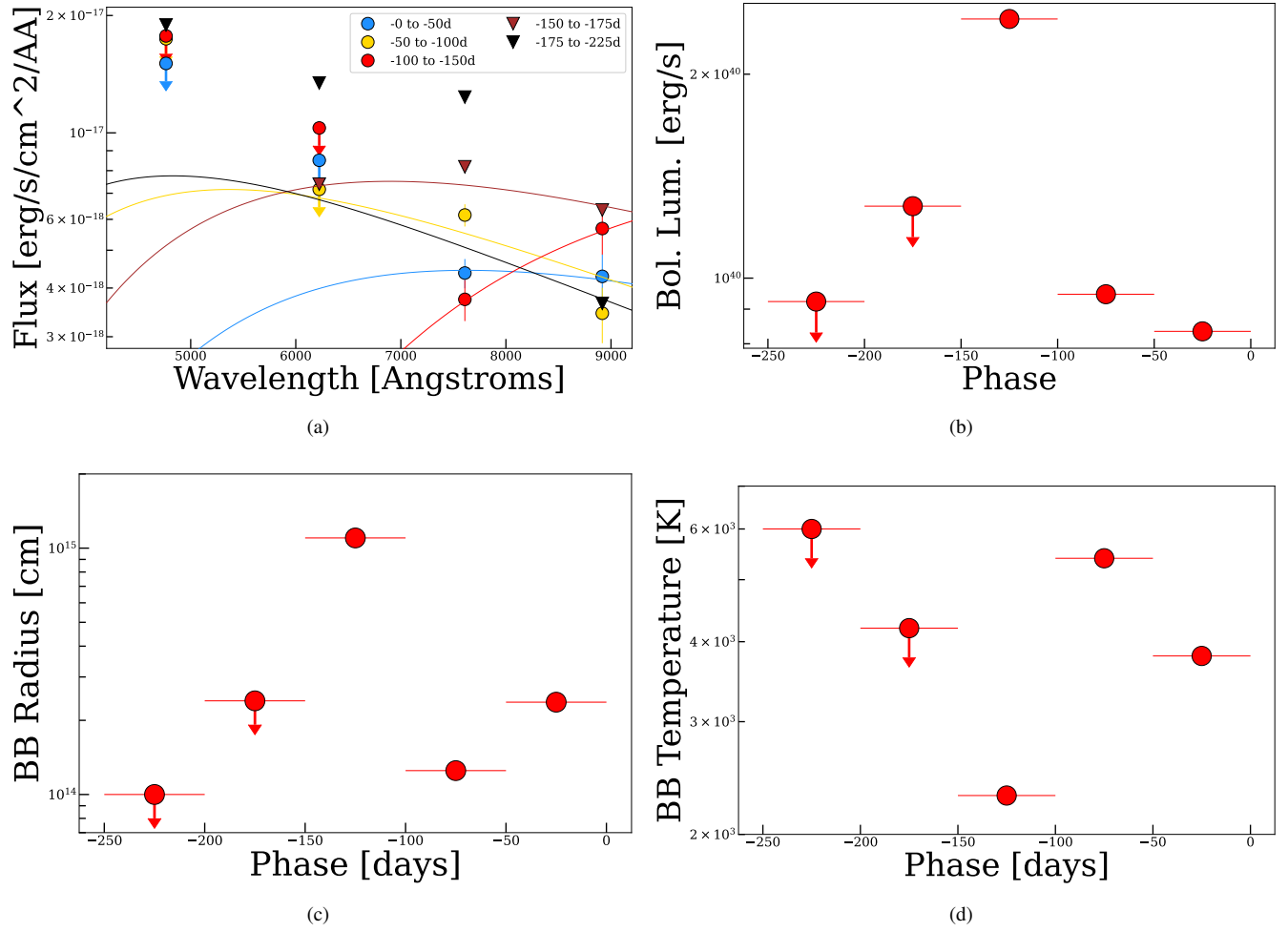


Figure 4. (a) Spectral energy distribution using *griz*-band limits and detections in 50 day pre-SN light curve bins. Best-fitting blackbody models shown as solid lines. Pre-explosion (a) bolometric luminosity, (b) blackbody radius, and (c) blackbody temperature as a function of phase. These parameters were derived from blackbody model fits to the 50 day binned SED.

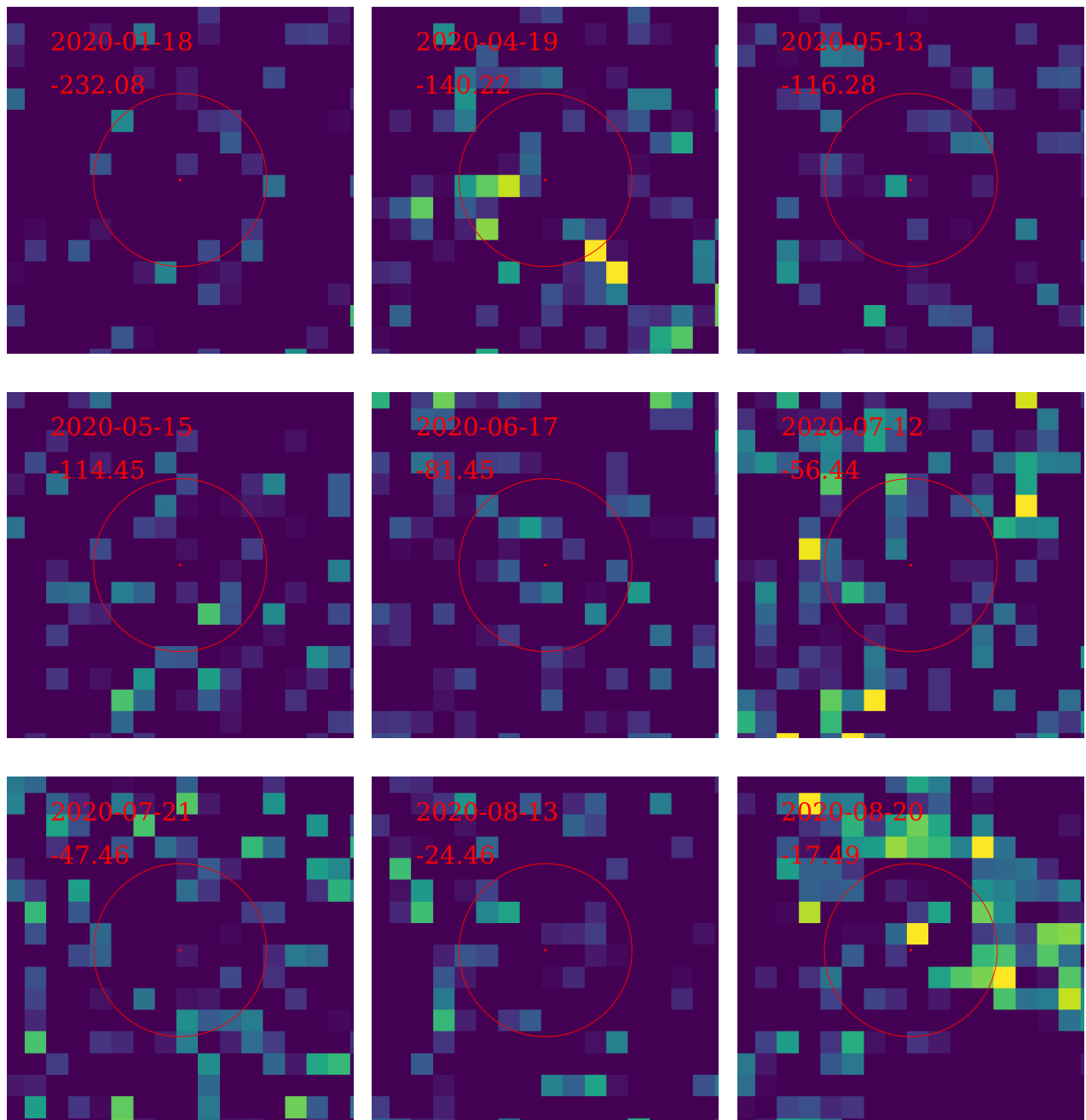


Figure 5. Pan-STARRS g-band pre-explosion images of SN 2020tlf. Images with pre-SN emission detected at above 80 and 50% recovery levels labeled with cyan and magenta, respectively.

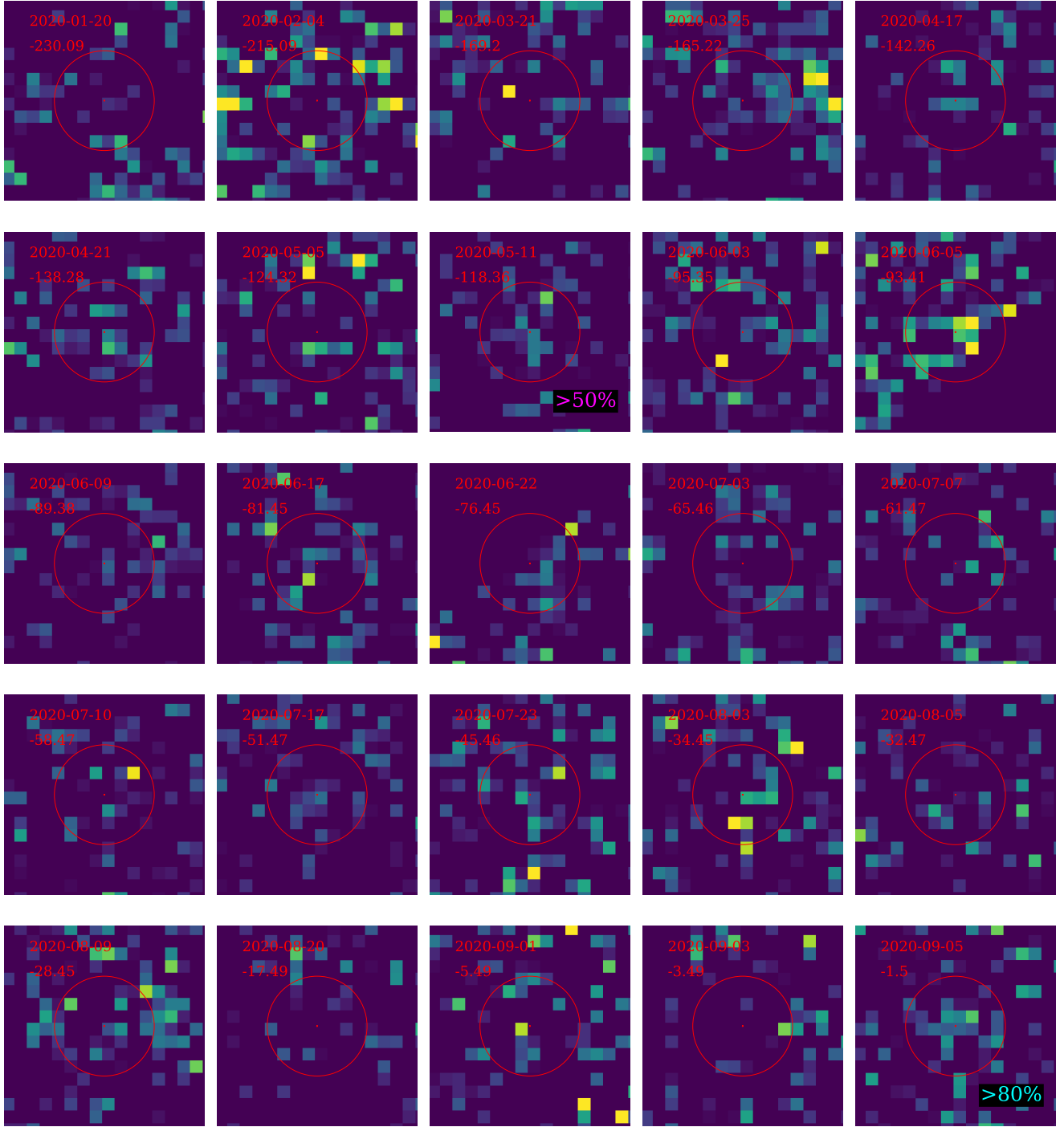


Figure 6. Pan-STARRS *r*-band pre-explosion images of SN 2020tlf. Images with pre-SN emission detected at above 80 and 50% recovery levels labeled with cyan and magenta, respectively.

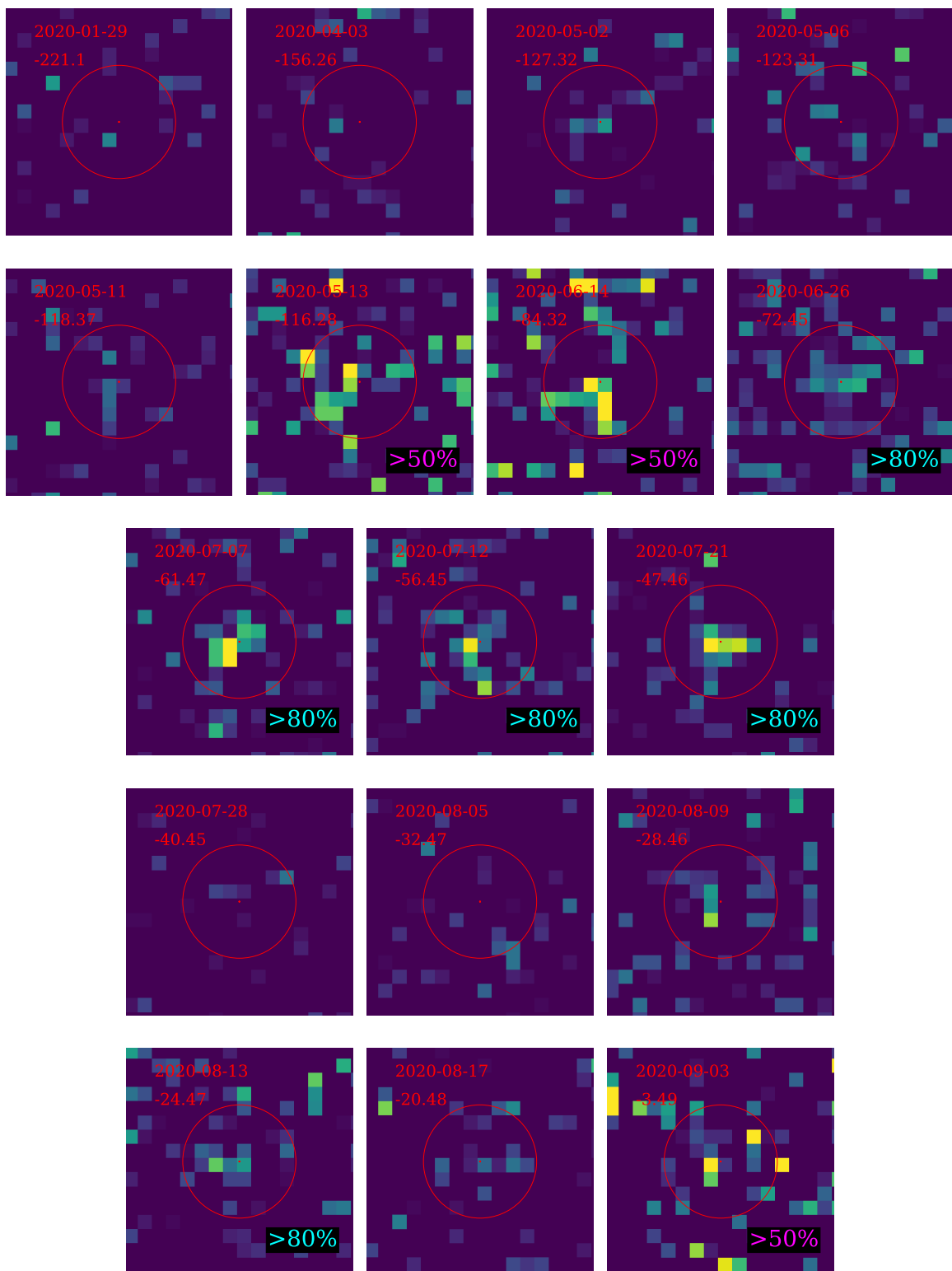


Figure 7. Pan-STARRS *i*-band pre-explosion images of SN 2020tlf. Images with pre-SN emission detected at above 80 and 50% recovery levels labeled with cyan and magenta, respectively.

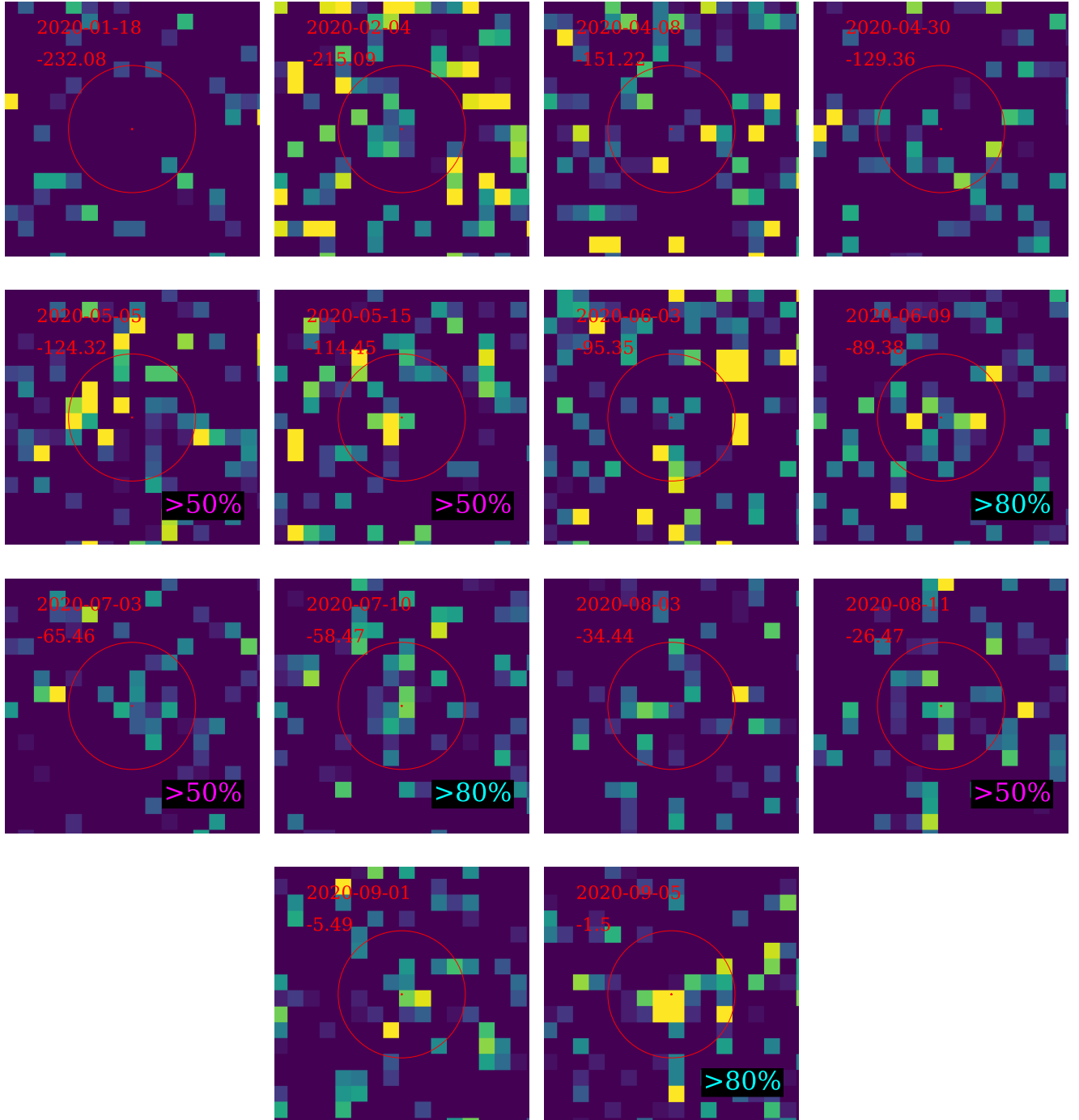


Figure 8. Pan-STARRS z-band pre-explosion images of SN 2020tlf. Images with pre-SN emission detected at above 80 and 50% recovery levels labeled with cyan and magenta, respectively.

Table 1. Pre-SN PS1/YSE Photometry of SN 2020tlf

MJD	Phase ^a	Filter	Magnitude	Uncertainty	Recovery Efficiency
58866.7	-232.1	<i>g</i>	21.9	—	< 50%
58958.5	-140.2	<i>g</i>	22.0	—	< 50%
58982.5	-116.3	<i>g</i>	21.8	—	< 50%
58984.3	-114.4	<i>g</i>	22.2	—	< 50%
59017.3	-81.4	<i>g</i>	22.0	—	< 50%
59042.3	-56.4	<i>g</i>	22.3	—	< 50%
59051.3	-47.5	<i>g</i>	22.2	—	< 50%
59074.3	-24.5	<i>g</i>	21.8	—	< 50%
59081.2	-17.5	<i>g</i>	21.8	—	< 50%
58868.7	-230.1	<i>r</i>	21.8	—	< 50%
58929.5	-169.2	<i>r</i>	21.7	—	< 50%
58933.5	-165.2	<i>r</i>	21.8	—	< 50%
58974.4	-124.3	<i>r</i>	21.4	—	< 50%
58980.4	-118.4	<i>r</i>	21.8	0.3	> 50%
59003.4	-95.3	<i>r</i>	20.8	—	< 50%
59005.3	-93.4	<i>r</i>	21.2	—	< 50%
59009.4	-89.4	<i>r</i>	22.0	—	< 50%
59017.3	-81.4	<i>r</i>	22.1	—	< 50%
59033.3	-65.5	<i>r</i>	21.7	—	< 50%
59037.3	-61.5	<i>r</i>	22.2	—	< 50%
59040.3	-58.5	<i>r</i>	21.9	—	< 50%
59047.3	-51.5	<i>r</i>	21.2	—	< 50%
59053.3	-45.5	<i>r</i>	21.8	—	< 50%
59064.3	-34.4	<i>r</i>	21.3	—	< 50%
59066.3	-32.5	<i>r</i>	21.8	—	< 50%
59070.3	-28.4	<i>r</i>	21.6	—	< 50%
59081.2	-17.5	<i>r</i>	21.6	—	< 50%
59093.2	-5.5	<i>r</i>	21.3	—	< 50%
59095.2	-3.5	<i>r</i>	21.7	—	< 50%
59097.2	-1.5	<i>r</i>	21.4	0.2	> 80%

^aRelative to first light (MJD 59098.74)

Table 2. Pre-SN PS1/YSE Photometry of SN 2020tlf (cont.)

MJD	Phase ^a	Filter	Magnitude	Uncertainty	Recovery Efficiency
58877.6	-221.1	<i>i</i>	21.4	–	< 50%
58942.5	-156.3	<i>i</i>	20.8	–	< 50%
58971.4	-127.3	<i>i</i>	21.7	–	< 50%
58975.4	-123.3	<i>i</i>	21.6	–	< 50%
58980.4	-118.4	<i>i</i>	21.9	–	< 50%
58982.5	-116.3	<i>i</i>	21.4	0.3	> 50%
59014.4	-84.3	<i>i</i>	21.5	0.3	> 50%
59026.3	-72.4	<i>i</i>	21.1	0.2	> 80%
59037.3	-61.5	<i>i</i>	21.3	0.2	> 80%
59042.3	-56.4	<i>i</i>	21.3	0.2	> 80%
59051.3	-47.5	<i>i</i>	21.3	0.1	> 80%
59058.3	-40.4	<i>i</i>	21.5	–	< 50%
59066.3	-32.5	<i>i</i>	21.7	0.4	> 50%
59070.3	-28.5	<i>i</i>	21.1	–	< 50%
59074.3	-24.5	<i>i</i>	21.6	0.3	> 80%
59078.3	-20.5	<i>i</i>	21.8	–	< 50%
59095.2	-3.5	<i>i</i>	21.7	0.3	> 50%
58866.7	-232.1	<i>z</i>	21.6	–	< 50%
58883.7	-215.1	<i>z</i>	21.4	–	< 50%
58947.5	-151.2	<i>z</i>	21.1	–	< 50%
58969.4	-129.4	<i>z</i>	20.8	–	< 50%
58974.4	-124.3	<i>z</i>	20.7	0.3	> 50%
58984.3	-114.4	<i>z</i>	21.3	0.3	> 50%
59003.4	-95.3	<i>z</i>	20.4	–	< 50%
59009.4	-89.4	<i>z</i>	20.9	0.3	> 80%
59028.3	-70.5	<i>z</i>	21.6	–	< 50%
59033.3	-65.5	<i>z</i>	21.4	0.4	> 50%
59040.3	-58.5	<i>z</i>	21.1	0.3	> 80%
59064.3	-34.4	<i>z</i>	21.2	–	< 50%
59072.3	-26.5	<i>z</i>	21.3	0.4	> 50%
59093.2	-5.5	<i>z</i>	21.2	–	< 50%
59097.2	-1.5	<i>z</i>	20.7	0.2	> 80%

^aRelative to first light (MJD 59098.74)